*Journal of*
*Computational and Theoretical Nanoscience*
Vol. 9, 1596–1602, 2012

# Modeling of Drain Current for Grooved-Gate MOSFET

Jatmiko Endro Suseno[1,3], Sohail Anwar[2], Munawar Agus Riyadi[1,4], and Razali Ismail[1,*]

[1] *Faculty of Electrical Engineering, Universiti Teknologi Malaysia, Skudai, Johor, Malaysia*
[2] *Altoona College, Pennsylvania State University, USA*
[3] *Faculty of Mathematics and Natural Sciences, Department of Physics, Diponegoro University, Indonesia*
[4] *Faculty of Engineering, Department of Electrical Engineering, Diponegoro University, Indonesia*

A drain current model of grooved-gate MOSFET which is based on the difference of the channel depth distance along the channel from the source to the drain in cylindrical coordinate is presented in this paper. From the analysis, the potential of grooved-gate is related to geometry structure parameters the angle ($\theta_0$) and radius ($r_0$) of concave corner as well as channel depth ($d$). The presence of corner effect will influence to the drain potential, drain current characteristics as well as the other electrical characteristics, such as conductance ($g_m$) and transconductance ($g_d$). In this result, model shows effect of corner with improvement of the device the characteristics especially the reduction of short channel effect (SCE) althought drain current value grooved-gate MOSFET of is slightly less than the ordinary MOSFET.

**Keywords:** Grooved-Gate MOSFET, Curved Channel, Drain Current Model, Short Channel Effect (SCE), Potential Barrier.

## 1. INTRODUCTION

The small geometry of conventional bulk silicon MOSFETs into nanoscale regime has many problem of short-channel effects (SCEs). The grooved-gate MOSFET, which is created by corner region has a promising structure to reduce the Short Channel Effect. The influence of the corner effect may affect the potential barriers for the device channel[1,2] which can improve the characteristics of the device especially the reduction of short channel effect (SCE) such as a high threshold voltage ($V_{\text{th}}$), a low DIBL and GIDL effect, closeness to ideal sub-threshold slope, and a high $I_{\text{ON}}$–$I_{\text{OFF}}$ ratio.[1–6] While analytical numerical model of surface potential on Grooved-Gate MOSFET have been made using 2D Poisson equation method in cylindrical coordinates [*l*] which potential distribution function along channel, $V(\theta)$ elates into the grooved-gate MOSFET structural parameters ($r_0$, $\theta_0$, and $d$), substrate doping and applied biases.

In this paper, we present a new drain current model for drain current characteristics of grooved-gate MOSFET based on determination of channel depth at their respective angle in cylindrical coordinate. The model is approximation of geometrical structure in cylindrical coordinate which has curved region geometry which is going to be incapable of accurately simulating the $I$–$V$ characteristics of grooved-gate MOSFET including corner radius ($r_0$), corner angle ($\theta_0$), channel depth ($d$), channel length ($L_g$) and their relationship for the derivation of drain current, as well as conductance and transconductance.

## 2. STRUCTURE OF THE DEVICE

The grooved-gate MOSFET structure with depletion region is shown in Figure 1. In the device, the gate electrode is placed on a groove separating the source and drain region. In order to form the effective minus junction depth, the source/drain junction is made shallower than the groove bottom.

The presence of the groove in recessed-channel or grooved-gate MOSFETs can enhance the electrial performance.[8] The curved structure at the channel of device is effective in reducing the electric field at the drain, thus improving reliability. Furthermore, it can also reduce the substrate current, and increase the highest applicable gate to drain voltage, so that improving the reliability of the device.

The main advantage of groove-gate MOSFETs is the presence of large number of structral parameters, such as the concave corner radius, junction depth, the angle of the vertical concave sidewall structure and the channel doping concentration. These parameters can be used to adjust any short-channel effects, including sub-threshold swing ($S$), minimum surface potential, DIBL and threshold voltage roll-off, etc., whereas only the channel doping concentration can be used in conventional planar MOSFETs.

---

[*] Author to whom correspondence should be addressed.

1546-1955/2012/9/1596/007 doi:10.1166/jctn.2012.2250

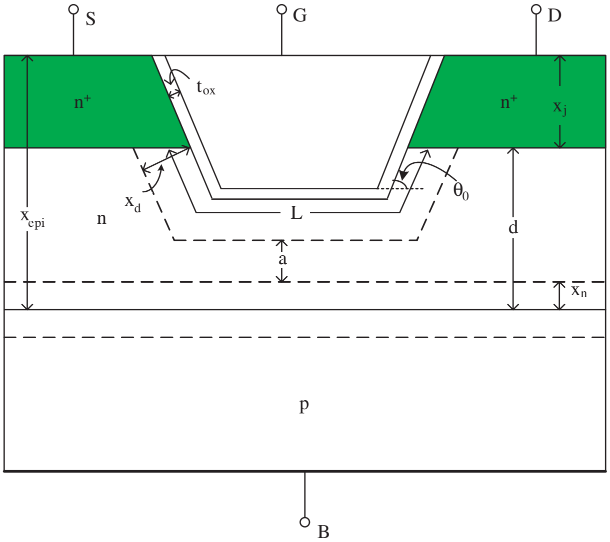

**Fig. 1.** The grooved-gate MOSFET structure.

## 3. MODEL OF DEVICE STRUCTURE

The grooved-gate MOSFET has the large number of structural parameters, such as the concave corner radius, junction depth, the angle of the vertical concave sidewall structure and the channel doping concentration. The variation of these parameters can improve the performace and short-channel effect (SCE). The grooved-gate structure of device can be approximated as the concave corner which is parts of cylinder.[1] This device is shown in Figure 2 below.

The electron potential profile in the channel region which have concave corner, is derived by the Poisson equation in cylindrical coordinates. The potential distribution function along channel from analytical model solution[1] has been derived as

$$V(\theta) = V_{\text{BS}} - \frac{M}{2x_{\text{deff}}}(V_g - \varphi_s(\theta))(R_2 - r)^2 \tag{1}$$

where $M$ and $x_{\text{deff}}$ are constant, $M = (C_{\text{oxc}}/\varepsilon_{\text{Si}})$ and $x_{\text{deff}} = \sqrt{((2\varepsilon_{\text{Si}})/(qN_A))1.5V_{\text{bi}}}$, respectively, and $C_{\text{oxc}}$ is the gate oxide capacitance per unit area[6] of corner region of the groove-gate, with $C_{\text{oxc}} = (\varepsilon_o \varepsilon_{\text{ox}})/(r_0 \ln(1 + t_{\text{ox}}/r_0))$.

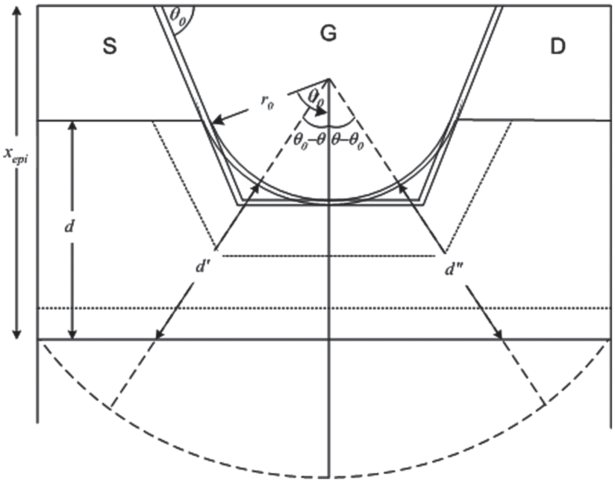

**Fig. 2.** The grooved-gate MOSFET with cylindrical approximtion of concave corner.

The modification of the potential equation at (1) using derivation of Poisson equation (as shown at Appendix A) we obtaine

$$V(\theta) = \text{Csch}\left(\frac{2\theta_0}{\lambda}\right)\left((\zeta + (V_d + \phi_{\text{SG}}))\text{Sinh}\left(\frac{\theta}{\lambda}\right) + (\zeta + \phi_{\text{SG}})\text{Sinh}\left(\frac{2\theta_0 - \theta}{\lambda}\right)\right) - \zeta \tag{2}$$

Where $\lambda$ and $\zeta$ are constants, $\lambda = x_{\text{deff}}\sqrt{2/(x_{\text{deff}} - R_1)}$ and $\zeta = -V_{\text{BS}} + (qN_A/\varepsilon_{\text{Si}})(2R_1 x_{\text{deff}}^2)/(R_1 - x_{\text{deff}})$, respectively.

## 4. MODEL OF *I–V* CHARACTERISTICS

The differential equation describing the $I$–$V$ characteristics of the device is given by:

$$I_d R_1\, d\theta = N_D q \mu_{\text{eff}} W a(\theta)\, dV(\theta) \tag{3}$$

where $W$ is the channel width, $\mu_{\text{eff}}$ is the effective electron mobility, $V_\theta(\theta)$ is the potential in the channel the potential component in the radial direction at angle $\theta$, and $a(\theta)$ is the effective channel depth distance along the channel from the source to the drain and is given by:

$$a(\theta) = d' - x_n(\theta) - x_d(\theta) \tag{4}$$

$d'$ is the effective geometrical channel depth, $x_d$ and $x_n$ are the depths of depletion regions of the MOS gate and the substrate respectively. This potential is zero at the source $(\theta = 0)$, and it is equal to $V_d$ at the drain $(\theta = 2\theta_0)$.

The depth of the depletion region $x_d$ associated with the MOS gate is given by:[10]

$$x_d = \frac{\varepsilon_{\text{Si}}}{2C_{\text{ox}}}((1 + \delta(V_g - V))^{1/2} - 1) \tag{5}$$

where $\delta$ is constant, $\delta = -(2C_{\text{oxc}}^2)/(\varepsilon_{\text{Si}} q N_D)$.

$N_D$ is the channel doping, $q$ is the electronic charge, and $\varepsilon_{\text{Si}}$ is the permittivity of silicon.

The depth of the substrate to channel depletion region $x_n$ is given by:[20]

$$x_n = K_o(\phi_{\text{bi}} + V_B + V(y))^{1/2} \tag{6}$$

where $K_o$ is constant, $K_o = ((2\varepsilon_{\text{Si}} N_A)/(qN_D(N_A + N_D)))^{1/2}$, $\phi_{\text{bi}} = (kT/q)\ln(N_A N_D/n_i^2)$ is the built-in potential, $V_B$ is the substrate voltage, $N_A$ and $N_D$ is the acceptor and donor concentration, respectively.

## 5. $I_d$–$V_{\text{ds}}$ CHARACTERISTICS

From Figure 2, the geometrical distance $d$ between the bottom of the groove and the metallurgical boundary of the

$p$–$n$ junction as well as by the depletion regions associated with the MOS gate and the substrate channel is

$$d = x_{\mathrm{epi}} - x_j \tag{7}$$

where $x_{\mathrm{epi}}$ is the thickness of the epitaxial layer and $x_j$ is the junction depth of the source/drain $n^+$ diffusion.

$$a(\theta) = \begin{cases} a'(\theta) = d' - x_d(\theta) - x_n(\theta) & 0 < \theta < \theta_0 \quad (8) \\ a''(\theta) = d'' - x_d(\theta) - x_n(\theta) & \theta_0 < \theta < 2\theta_0 \quad (9) \end{cases}$$

where: $d' = d\mathrm{Sec}(\theta_0 - \theta) - R_1\mathrm{Cos}(\theta_0)\mathrm{Sec}(\theta_0 - \theta) - R_1$, and $d'' = d\mathrm{Sec}(\theta - \theta_0) - R_1\mathrm{Cos}(\theta_0)\mathrm{Sec}(\theta - \theta_0) - R_1$.

$$I_d = \frac{N_D q \mu_n W}{2R_1\theta_0}\left[\int_{V(\theta=0)}^{V(\theta=\theta_0)} a'(\theta)dV(\theta) + \int_{V(\theta=\theta_0)}^{V(\theta=2\theta_0)} a''(\theta)dV(\theta)\right] \tag{10}$$

The above integration we obtain $I_d$–$V_d$ equation is

$$\begin{aligned} I_d = \frac{N_D q \mu_{\mathrm{eff}} W}{2R_1\theta_0}\Bigg[ & \frac{V_d\theta_0}{2\lambda}(d - R_1\mathrm{Cos}(\theta_0))\mathrm{Csch}\left(\frac{\theta_0}{\lambda}\right) \\ & + \frac{\theta_0}{\lambda}\mathrm{Csch}\left(\frac{2\theta_0}{\lambda}\right)(d\mathrm{Sec}(\theta_0) - R_1) \\ & \times\left((\phi_{SG} + V_d)\mathrm{Cosh}\left(\frac{2\theta_0}{\lambda}\right) - \phi_{\mathrm{SG}}\right) \\ & - R_1V_d + \frac{V_d\varepsilon_{\mathrm{Si}}}{C_{\mathrm{ox}}} + \frac{\varepsilon_{\mathrm{Si}}}{3C_{\mathrm{ox}}\delta} \\ & \times\left(1 - (V_d + \varphi_{\mathrm{SG}} - V_g)\delta\right)^{3/2} \\ & - \frac{2}{3}K_0(V_d + \varphi_{\mathrm{SG}} + V_B + \varphi_{bi})^{3/2} \\ & - \frac{\varepsilon_{\mathrm{Si}}}{3C_{\mathrm{ox}}\delta}\left(1 - (\varphi_{\mathrm{SG}} - V_g)\delta\right)^{3/2} \\ & + \frac{2}{3}K_0(\varphi_{\mathrm{SG}} + V_B + \varphi_{\mathrm{bi}})^{3/2}\Bigg] \end{aligned} \tag{11}$$

where $N_D$ is the channel doping, $q$ is the electronic charge, $\mu_n$ is the low field bulk mobility of electrons, $W$ is the channel width, $d$ is the effective geometrical channel depth, $\varepsilon_{\mathrm{Si}}$, $\varepsilon_0$ are the permittivity of silicon and silicon dioxide respectively and $t_{\mathrm{ox}}$ is the oxide thickness along the walls of the groove, $V_d$ is the drain voltage, $V_B$ is the substrate bias and $V_g$ is the effective gate voltage. The parameters $K_o$ and $\delta$ are the constants defined above.

The source–drain conductance $g_d$ can be found by differentiation of $I_d$ with respect to $V_d$ and is given by:

$$\begin{aligned} g_d = \left.\frac{dI_d}{dV_d}\right|_{V_d=0} = \frac{N_D q W \mu_{\mathrm{eff}}}{2R_1\theta_0} & \times\Bigg(d + \frac{\varepsilon_{\mathrm{Si}}}{C_{\mathrm{ox}}} - K_o\sqrt{V_{bs} - V_g + \phi_{\mathrm{bi}} + \phi_{\mathrm{SG}}} \\ & - \frac{\varepsilon_{\mathrm{Si}}}{2C_{\mathrm{ox}}}\sqrt{1 - \delta(\phi_{\mathrm{SG}} - V_g)}\Bigg) \end{aligned} \tag{12}$$

The transconductance in the saturation region $g_m$ is obtained by differentiation of $I_d$ with respect to $V_g$ in the saturation region:

$$\begin{aligned} g_m &= \left.\frac{dI_d}{dV_g}\right|_{V_d=V_{ds}} \\ &= \frac{N_D q W \mu_{\mathrm{eff}}}{2R_1\theta_0}\Bigg(K_o\sqrt{V_{bs} + V_{ds} - V_g + \phi_{\mathrm{bi}} + \phi_{\mathrm{SG}}} \\ &\quad - K_o\sqrt{V_{bs} - V_g + \phi_{\mathrm{bi}} + \phi_{\mathrm{SG}}} \\ &\quad - \frac{\varepsilon_{\mathrm{Si}}}{2C_{\mathrm{ox}}}\sqrt{1 - \delta(\phi_{\mathrm{SG}} - V_g)} \\ &\quad + \frac{\varepsilon_{\mathrm{Si}}}{2C_{\mathrm{ox}}}\sqrt{1 - \delta(V_{ds} + \phi_{\mathrm{SG}} - V_g)}\Bigg) \end{aligned} \tag{13}$$

## 6. RESULTS AND DISCUSSION

The $I_d$–$V_{\mathrm{ds}}$ characteristics can be obtained from Eq. (11) as shown Figure 3. This graph shows the current drain reduction compared with planar MOSFETs, due to the drain separation from the implanted channel region, as well as the curved structure at the drain is effective in reducing the electric field at the drain, thus improving reliability. This also decreases the substrate current, and increase the highest applicable gate to drain voltage, hence improving the reliability of the device.

Some researcher have done improvement in the drive curent with some treatment. One of them is using a hydrogen anneal at 800 °C that give a 30% improvement of the drive current at 120-nm $n$-channel transistors.[9]

The drain current graphs of device with various the concave corner are given in Figures 4 and 5 for various $\theta_0$ from 0° to 90°. The device with minimum angle of corner (0°) is like a planar device. These graphs show that the drain current increase obviously for a relatively bigger corner angle.

In other words, the presence of the corner effects can reduce the drain current due to the potential barrier for electron flow from source to drain will increase and then the potential barrier which is effective in suppresing the

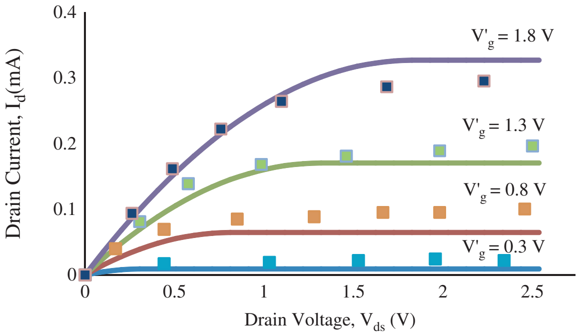

**Fig. 3.** $I_d$–$V_d$ characteristics of grooved-gate MOSFET, with $\theta_0 = 0.46\pi$ and $r_0 = 1.2$ nm.

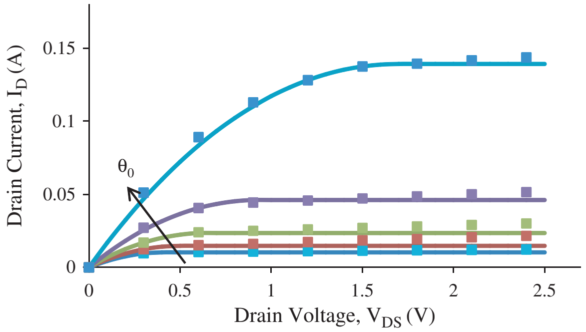

**Fig. 4.** $I_d$–$V_d$ graphs with various $\theta_0$ and $V_g = 1.3$ V.

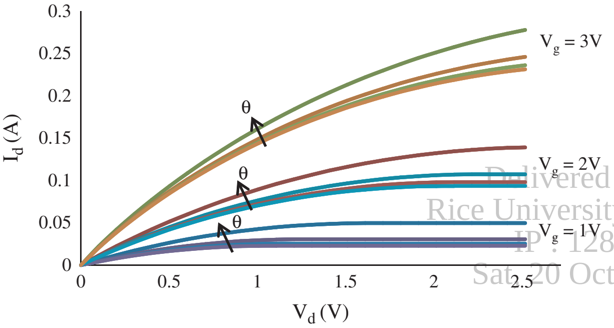

**Fig. 5.** $I_d$–$V_d$ graphs with various $\theta_0$ and $V_g$.

short channel effect degrades the dran current characteristics as compared with the planar device.

Figure 6 shows a typical set of $I$–$V$ characteristic curves for the grooved-gate MOSFET geometry with various geometric channel depths $d$. The graph shows the drain current increase with channel depth $d$ increase for all gate voltage values. It means that device with the smaller $d$ has easy to complete MOS gate pinch-off and for higher $d$, the saturation of drain current does occur although the gate pinch-off may not occur.

While the pinched-off devices, there are electrical characteristics measurements include $I$–$V$ characteristics, conductance below saturation, transconductance in the saturation region, pinch-off voltage and etc. For grooved-gate, the transconductance ($g_m$) and conductance ($g_d$) are very corelated with device geometry especially corner angle due to effect to depletion shape when pinch off does occur. The Figure 7 shows graphs of normalized the transconductance ($g_m$) and conductance ($g_d$) with normalized angle of corner. The transconductance $g_m$ increases exponentially as the corner angle of device increases. In contras with it, the conductance ($g_d$) decrease linearly when angle of corner inreases.

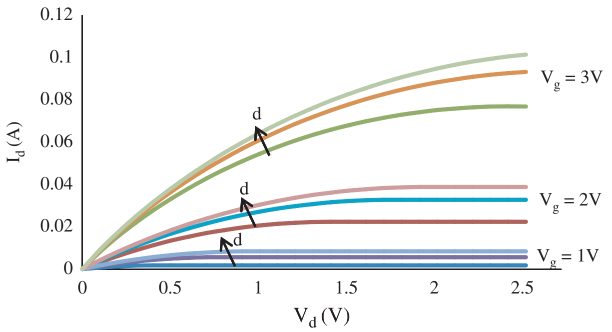

**Fig. 6.** $I_d$–$V_d$ Characteristics with various $d$ and $V_g$.

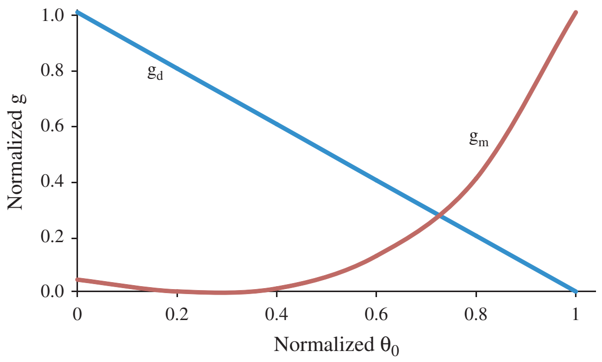

**Fig. 7.** The graphs of normalized of conductance ($g_d$) and transconductance ($g_m$) of device as various normalized $\theta_0$.

These results are obtained directly from solving Eqs. (12) and (13) instead of using the modulation of normalized $\theta_0$ which assumes that the effective channel length decreases with drain voltage increases beyond saturation when pinch off does occur.

## 7. CONCLUSION

This drain current model of grooved-gate MOSFET is based on the channel depth distance along the channel using 2D Poisson equation solution in cylidrical coordinates. The structure includes some parameters, such as the concave corner radius, junction depth, the angle of the vertical concave sidewall structure and the channel doping concentration.

The result shows any reduction of the drain current due to the potential barrier from the implanted channel region and the curved structure. Furthermore, it is effective in reducing the electric field at the drain, thus improving reliability of short channel effects (SCEs), such as including sub-threshold swing ($S$), minimum surface potential, DIBL and threshold voltage roll-off, etc. For drain current current reduction, it has been done fabrication using experiment of a hydrogen anneal at 800 °C that gives a 30% improvement of the drive current at the device.

## APPENDICES

### Appendix A. Derivation of Potential Equation

The analytical model of grooved-gate potential have been modelled by Ref. [1], it is

$$V(\theta) = V_{\text{BS}} - \frac{M}{2x_{\text{deff}}}(V_g - \varphi_s(\theta))(R_2 - r)^2 \qquad \text{(A1)}$$

$$\frac{dV(r,\theta)}{dr} = \frac{M}{x_{\text{deff}}}(V_g - \varphi_s(\theta))(R_2 - r) \tag{A2}$$

$$\frac{\partial^2 V(r,\theta)}{\partial r^2} = -\frac{M}{x_{\text{deff}}}(V_g - \varphi_s(\theta)) \tag{A3}$$

The Poisson equaion

$$\frac{\partial^2 V(r,\theta)}{\partial r^2} + \frac{1}{r}\frac{\partial V(r,\theta)}{\partial r} + \frac{1}{r^2}\frac{\partial^2 V(r,\theta)}{\partial \theta^2} = \frac{qN_A}{\varepsilon_{\text{Si}}} \tag{A4}$$

$$-\frac{M}{x_{\text{deff}}}(V_g - \varphi_s(\theta)) + \frac{M}{r\,x_{\text{deff}}}(V_g - \varphi_s(\theta))(R_2 - r) + \frac{1}{r^2}\frac{\partial^2 V(r,\theta)}{\partial \theta^2} = \frac{qN_A}{\varepsilon_{\text{Si}}} \tag{A5}$$

$$\frac{\partial^2 V(r,\theta)}{\partial \theta^2} - \frac{r^2 qN_A}{\varepsilon_{\text{Si}}} - \frac{M}{x_{\text{deff}}} \times (V_g - \varphi_s(\theta))(2r^2 - rR_2) = 0 \tag{A6}$$

From Eq. (1) we have

$$\frac{M}{x_{\text{deff}}}(V_g - \varphi_s(\theta)) = \frac{V_{\text{BS}} - V(r,\theta)}{2(r-R_2)^2} \tag{A7}$$

$$\frac{\partial^2 V(r,\theta)}{\partial \theta^2} - \frac{r^2 qN_A}{\varepsilon_{\text{Si}}} - \frac{r(2r-R_2)}{2(r-R_2)^2}(V_{\text{BS}} - V(r,\theta)) = 0 \tag{A8}$$

Using Poisson equation above, the potential Eq. (A1) can be simplified through assumption of potential at surface of the channel, with $r = R_1 = r_o + t_{\text{ox}}$

$$\frac{\partial^2 V(\theta)}{\partial \theta^2} - \frac{R_1^2 qN_A}{\varepsilon_{\text{Si}}} + \frac{R_1(x_{\text{deff}} - R_1)}{2x_{\text{deff}}^2}(V_{\text{BS}} - V(\theta)) = 0 \tag{A9}$$

$$\frac{\partial^2 \Phi(\theta)}{\partial \theta^2} - \frac{\Phi(\theta)}{\lambda^2} = 0 \tag{A10}$$

where $\lambda^2 = (2x_{\text{deff}}^2)/(x_{\text{deff}} - R_1)$

$$\Phi(\theta) = V(\theta) - V_{\text{BS}} + \frac{qN_A}{\varepsilon_{\text{Si}}}\frac{2R_1 x_{\text{deff}}^2}{(R_1 - x_{\text{eff}})} \tag{A11}$$

Assume that

$$\zeta = -V_{\text{BS}} + \frac{qN_A}{\varepsilon_{\text{Si}}}\frac{2R_1 x_d^2}{(R_1 - x_{\text{deff}})}$$

$$\Phi(\theta) = \zeta + V(\theta) \tag{A12}$$

The boundary conditions are $V(\theta = 0) = \phi_{\text{SG}}$ and $V(\theta = 2\theta_0) = V_d + \phi_{\text{SG}}$, with $\phi_{\text{SG}}$ is the potential at surface for the grooved-gate. Therefore, the solution to Eq. (A4) is

$$\Phi(0) = \zeta + \phi_{\text{SG}} \tag{A13}$$

$$\Phi(2\theta) = \zeta + (V_d + \phi_{\text{SG}}) \tag{A14}$$

$$\Phi(\theta) = \text{Csch}\left(\frac{2\theta_0}{\lambda}\right)\left((\zeta + (V_d + \phi_{\text{SG}}))\text{Sinh}\left(\frac{\theta}{\lambda}\right) + (\zeta + \phi_{\text{SG}})\text{Sinh}\left(\frac{2\theta_0 - \theta}{\lambda}\right)\right) \tag{A15}$$

From Eq. (A13) we have the potential is

$$V(\theta) = \Phi(\theta) - \zeta \tag{A16}$$

$$V(\theta) = \text{Csch}\left(\frac{2\theta_0}{\lambda}\right)\left((\zeta + (V_d + \phi_{\text{SG}}))\text{Sinh}\left(\frac{\theta}{\lambda}\right) + (\zeta + \varphi_{\text{SG}})\text{Sinh}\left(\frac{2\theta_0 - \theta}{\lambda}\right)\right) - \zeta \tag{A17}$$

## Appendix B. Derivation of the Effective Channel Depth $d'$ and $d''$

$$n = R_1\text{Cos}(\theta_0) \tag{B1}$$

$$k = (d + n)\text{Sec}(\theta_0) = d\text{Sec}(\theta_0) + R_1 \tag{B2}$$

(a) Determination of $d'$

$$l' = k\text{Cos}(\theta_0 - \theta) = (d\text{Sec}(\theta_0) + R_1)\text{Cos}(\theta_0 - \theta) \tag{B3}$$

$$m' = l' - d - n = (d\text{Sec}(\theta_0) + R_1)\text{Cos}(\theta_0 - \theta) - d - R_1\text{Cos}(\theta_0) \tag{B4}$$

$$d' = k - m\text{Sec}(\theta_0 - \theta) - R_1 = d\text{Sec}(\theta_0 - \theta) - R_1\text{Cos}(\theta_0)\text{Sec}(\theta_0 - \theta) - R_1 \tag{B5}$$

(b) Determination of $d''$

$$l'' = k\text{Cos}(\theta - \theta_0) = (d\text{Sec}(\theta_0) + R_1)\text{Cos}(\theta - \theta_0) \tag{B6}$$

$$m'' = l'' - d - n = (d\text{Sec}(\theta_0) + R_1)\text{Cos}(\theta - \theta_0) - d - R_1\text{Cos}(\theta_0) \tag{B7}$$

$$d'' = k - m\text{Sec}(\theta - \theta_0) - R_1 = d\text{Sec}(\theta - \theta_0) - R_1\text{Cos}(\theta_0)\text{Sec}(\theta - \theta_0) - R_1 \tag{B8}$$

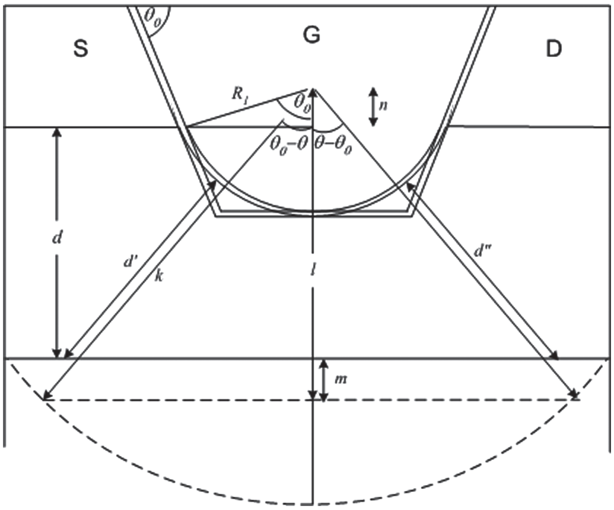

**Fig. B1.** The grooved-gate MOSFET structure with its parameters for $d'$ and $d''$ measurement.

## Appendix C. Derivation of Drain Current Equation

The potential equation for grooved-gate structure is

$$\begin{aligned} V(\theta) = \mathrm{Csch}\left(\frac{2\theta_0}{\lambda}\right)\Bigg((\zeta+(V_d+\phi_{\mathrm{SG}}))\mathrm{Sinh}\left(\frac{\theta}{\lambda}\right) \\ +(\zeta+\phi_{\mathrm{SG}})\mathrm{Sinh}\left(\frac{2\theta_0-\theta}{\lambda}\right)\Bigg)-\zeta \end{aligned} \tag{C1}$$

where $\zeta = -V_{\mathrm{BS}} + ((qN_A)/\varepsilon_{\mathrm{Si}})((2R_1x_d^2)/(R_1 - x_{\mathrm{deff}}))$.

The potential values at locations of 0, $\theta_0$, and $2\theta_0$ are

$$V_0 = V(0) = \phi_{\mathrm{SG}} \tag{C2}$$

$$\begin{aligned} V_1 &= V(\theta_0) \\ &= (\zeta+V_d+2\phi_{\mathrm{SG}})\mathrm{Sinh}\left(\frac{\theta_0}{\lambda}\right)\mathrm{Csch}\left(\frac{2\theta_0}{\lambda}\right)-\zeta \end{aligned} \tag{C3}$$

$$V_2 = V(2\theta_0) = (V_d+\phi_{\mathrm{SG}}) \tag{C4}$$

From Eq. (10) we have

$$\begin{aligned} I_d = \frac{N_Dq\mu_nW}{2R_1\theta_0}\Bigg[\int_{V(\theta=0)}^{V(\theta=\theta_0)} a'(\theta)dV(\theta) \\ +\int_{V(\theta=\theta_0)}^{V(\theta=2\theta_0)} a''(\theta)dV(\theta)\Bigg] \end{aligned} \tag{C5}$$

$$\begin{aligned} I_d = {} & \frac{N_Dq\mu_nW}{2R_1\theta_0} \\ & \times\Bigg[\int_{\theta=0}^{\theta=\theta_0}\Bigg((d\mathrm{Sec}(\theta_0-\theta)-R_1\mathrm{Cos}(\theta_0) \\ & \times\mathrm{Sec}(\theta_0-\theta)-R_1)\frac{dV(\theta)}{d\theta}\Bigg)d\theta \\ & -\int_{V(\theta=0)}^{V(\theta=\theta_0)}(R_1+x_d(\theta)+x_n(\theta))dV(\theta) \\ & +\int_{\theta=\theta_0}^{\theta=2\theta_0}\Bigg((d\mathrm{Sec}(\theta-\theta_0)-R_1\mathrm{Cos}(\theta_0) \\ & \times\mathrm{Sec}(\theta-\theta_0)-R_1)\frac{dV(\theta)}{d\theta}\Bigg)d\theta \\ & -\int_{V(\theta=\theta_0)}^{V(\theta=2\theta_0)}(R_1+x_d(\theta)+x_n(\theta))dV(\theta)\Bigg] \end{aligned} \tag{C6}$$

The differential of potential Eq. (C1) by $\theta$ is

$$\begin{aligned} \frac{dV(\theta)}{d\theta} = \frac{1}{\lambda}\mathrm{Csch}\left(\frac{2\theta_0}{\lambda}\right)\Bigg((\zeta+V_d+\phi_{\mathrm{SG}})\mathrm{Cosh}\left(\frac{\theta}{\lambda}\right) \\ -(\zeta+\phi_{\mathrm{SG}})\mathrm{Cosh}\left(\frac{2\theta_0-\theta}{\lambda}\right)\Bigg) \end{aligned} \tag{C7}$$

Equation (C11) substituted into Eq. (C10) as

$$\begin{aligned} I_d = {} & \frac{N_Dq\mu_nW}{2R_1\theta_0} \\ & \times\Bigg[\mathrm{Csch}\left(\frac{2\theta_0}{\lambda}\right)\int_{\theta=0}^{\theta=\theta_0}\Bigg(((d\mathrm{Sec}(\theta_0-\theta)-R_1\mathrm{Cos}(\theta_0) \\ & \times\mathrm{Sec}(\theta_0-\theta)))\Bigg((\zeta+(V_d+\phi_{\mathrm{SG}}))\mathrm{Cosh}\left(\frac{\theta}{\lambda}\right) \\ & -(\zeta+\phi_{\mathrm{SG}})\mathrm{Cosh}\left(\frac{2\theta_0-\theta}{\lambda}\right)\Bigg)\Bigg)d\theta \\ & -\int_{V=V_0}^{V=V_1}\Bigg(R_1+K_o(\phi_{\mathrm{bi}}+V_B+V(\theta))^{1/2} \\ & +\frac{\varepsilon_{\mathrm{Si}}}{2C_{\mathrm{ox}}}((1+\delta(V_g-V(\theta)))^{1/2}-1)\Bigg)dV(\theta) \\ & +\mathrm{Csch}\left(\frac{2\theta_0}{\lambda}\right)\int_{\theta=\theta_0}^{\theta=2\theta_0}\Bigg(((d\mathrm{Sec}(\theta_0-\theta)-R_1 \\ & \times\mathrm{Cos}(\theta_0)\mathrm{Sec}(\theta-\theta_0)))\Bigg((\zeta+(V_d+\phi_{\mathrm{SG}})) \\ & \times\mathrm{Cosh}\left(\frac{\theta}{\lambda}\right)-(\zeta+\phi_{\mathrm{SG}})\mathrm{Cosh}\left(\frac{2\theta_0-\theta}{\lambda}\right)\Bigg)\Bigg)d\theta \\ & -\int_{V=V_1}^{V=V_2}\Bigg(R_1+K_o(\phi_{\mathrm{bi}}+V_B+V(\theta))^{1/2} \\ & +\frac{\varepsilon_{\mathrm{Si}}}{2C_{\mathrm{ox}}}((1+\delta(V_g-V(\theta)))^{1/2}-1)\Bigg)dV(\theta)\Bigg] \end{aligned} \tag{C8}$$

$$\begin{aligned} I_d = {} & \frac{N_Dq\mu_nW}{2R_1\theta_0} \\ & \times\Bigg[\frac{\theta_0}{2\lambda}\Bigg(V_d(d-R_1\mathrm{Cos}(\theta_0))\mathrm{Csch}\left(\frac{\theta_0}{\lambda}\right) \\ & +2(d\mathrm{Sec}(\theta_0)-2R_1)((\zeta+\phi_{\mathrm{SG}}+V_d) \\ & \times\mathrm{Cotanh}\left(\frac{2\theta_0}{\lambda}\right)-(\zeta+\phi_{\mathrm{SG}})\mathrm{Csch}\left(\frac{2\theta_0}{\lambda}\right)\Bigg) \\ & -R_1V_d+\frac{V_d\varepsilon_{\mathrm{Si}}}{C_{\mathrm{ox}}}+\frac{\varepsilon_{\mathrm{Si}}}{3C_{\mathrm{ox}}\delta}(1-(V_d+\phi_{\mathrm{SG}}-V_g)\delta)^{3/2} \\ & -\frac{2}{3}K_0(V_d+\phi_{\mathrm{SG}}+V_B+\phi_{\mathrm{bi}})^{3/2} \\ & -\frac{\varepsilon_{\mathrm{Si}}}{3C_{\mathrm{ox}}\delta}(1-(\phi_{\mathrm{SG}}-V_g)\delta)^{3/2} \\ & +\frac{2}{3}K_0(\phi_{\mathrm{SG}}+V_B+\phi_{\mathrm{bi}})^{3/2} \end{aligned} \tag{C9}$$

## References

1. Z. X. Ju, G. Xin, W. J. Ping, and H. Yue, *Chin. Phys. Soc. IOP Publishing Ltd.* 15, 631 **(2006)**.
2. S. Kimura, J. Tanaka, H. Noda, T. Toyabe, and S. Ihara, *IEEE Transactions on Electron Devices* 42, 94 **(1995)**.
3. K. Rajendran and W. Schoenmaker, *Microelectron. J.* 32, 631 **(2001)**.
4. X. J. Zhang, X. H. Ma, H. X. Ren, Y. Hao, and B. G. Sun, Study on 0.1 micron grooved-gate CMOS, *Solid-State and Integrated Circuits*

*Technology, 2004, Proceedings, 7th International Conference*, IEEE Conference Publications, October **(2004)**, Vol. 1, pp. 126–129.

5. J. N. Tong, X. C. Zou, and X. B. Shen, *Chin. Phys. Soc. IOP Publishing Ltd.* 13, 1816 (**2004**).
6. P. H. Bricout and E. Dubois, *IEEE Transactions on Electron Devices* 43, 1251 **(1996)**.
7. P. H. Bricout and E. Dubois, *IEEE Transactions on Electron Devices* 43, 1251 **(1996)**.
8. J. Tanaka, T. Toyabe, S. Ihara, S. Kimura, H. Noda, and K. Itoh, *IEEE Electron Device Letters* 14, 396 **(1993)**.
9. M. M. A. Hakim, A. Abuelgasim, L. Tan, and C. H. de Groot, *IEEE Electron Device Letters* 32, 279 (**2011**).

Received: 29 July 2011. Accepted: 14 September 2011.